

## Article

# Long-Term Variability of Vegetation Cover and Its Driving Factors and Effects over the Zuli River Basin in Northwest China

Chenlu Huang <sup>1</sup>, Juan Xu <sup>2,\*</sup> and Linxin Shan <sup>3</sup>

<sup>1</sup> Institute of Human Geography, College of Tourist, Xi'an International Studies University, Xi'an 710127, China

<sup>2</sup> Information and Technology Equipment Support Center, Meteorological Bureau of Gansu Province, Lanzhou 730000, China

<sup>3</sup> New Surveying and Mapping Development Research Center, Xi'an Institute of Prospecting and Mapping, Xi'an 710054, China

\* Correspondence: juanxu\_nuist@163.com; Tel.: +86-15093727817

**Abstract:** Vegetation information is a critical factor in regional environment management under climate change. In this study, a typical arid and semi-arid watershed on the Loess Plateau, the Zu Li River Basin (ZRB), was selected to study the long-term changes in vegetation cover and its drivers and impacts. Unlike existing normalized vegetation index (NDVI) products, which have coarse spatial resolution and short time horizons, this study used the 30 m Landsat dataset analyzed in the Google Earth Engine (GEE) to generate high-resolution and long-term NDVI data, which are the most ideal for monitoring vegetation dynamics using long-time-series data products. The results showed that the annual mean maximum NDVI (normalized vegetation index) in the ZRB increased during 1987–2021, with a significant ( $p < 0.05$ ) increasing trend in most areas. Upstream vegetation cover increased more than midstream and downstream, but the increase was smaller. Precipitation in the ZRB area was significantly ( $p < 0.05$ ) correlated with the NDVI series, except for the upstream pass area, where human activities played an important role. NDVI was significantly ( $p < 0.05$ ) negatively correlated with runoff coefficient and sand content, indicating that vegetation cover was an important reason for the decrease in runoff coefficient and sand content.

**Keywords:** normalized difference vegetation index; Landsat; precipitation; human activities



**Citation:** Huang, C.; Xu, J.; Shan, L. Long-Term Variability of Vegetation Cover and Its Driving Factors and Effects over the Zuli River Basin in Northwest China. *Sustainability* **2023**, *15*, 1829. <https://doi.org/10.3390/su15031829>

Academic Editor: Alejandro Javier Rescia Perazzo

Received: 22 September 2022

Revised: 2 November 2022

Accepted: 12 January 2023

Published: 18 January 2023



**Copyright:** © 2023 by the authors. Licensee MDPI, Basel, Switzerland. This article is an open access article distributed under the terms and conditions of the Creative Commons Attribution (CC BY) license (<https://creativecommons.org/licenses/by/4.0/>).

## 1. Introduction

Vegetation is generally considered to be an important indicator of biodiversity and ecological processes [1], and is an important medium of water, material cycle, and energy balance [2,3]. The impact of global warming and population growth has resulted in significant changes in regional and global vegetation cover over the past few decades [4]. Therefore, a comprehensive study of long-term vegetation change is important for better understanding of the spatial and temporal changes in landscape and its regulation of regional ecosystem balance under environment changes over the past century [5].

Remote sensing technology allows the rapid and accurate detection of vegetation cover dynamics on different scales of space and time [6,7]. NDVI (normalized difference vegetation index) is the most widely used dynamic remote sensing spectral index of vegetation cover in the world [8]. For example, Du found a gradual decline in the rate of NDVI change over three decades from 1982 to 2012 for the growing and all seasons, as detected using the Global Inventory Monitoring and Modelling System (GIMMS) NDVI dataset [3]. According to the NDVI dataset of MODIS (Moderate-Resolution Imaging Spectroradiometer), Zhao found a significant increase in annual and seasonal NDVI between 2000 and 2014, and claimed that the Grain for Green Project (GGP) had had a significant impact on NDVI, leading to strong correlations between the accumulated afforestation area and annual NDVI in Yan'an and Yulin [9].

The above studies were mainly based on low-resolution images such as the GIMMS-NDVI dataset and MODIS-NDVI dataset. In addition, most studies have focused only on the driving factors of vegetation cover, and the effects of vegetation cover on runoff and sediment transport have been neglected. In addition, the obvious changes in vegetation cover have a significant impact on physical and ecological processes [10,11], such as the change in surface energy balance, and the impact on soil erosion processes. Specifically, improvements in vegetation cover can reduce runoff by intercepting slope flow and increasing infiltration time [12]; at the same time, the kinetic energy of raindrops can be reduced by increasing the protection capacity of the soil surface, thus affecting the sediment source in the basin [13]. On the basis of the above discussion, this study focuses on the impact of NDVI changes on runoff and sediment transport in the past few decades.

In addition, the Loess Plateau is the area with the most serious soil erosion in China [14,15]. In order to control soil erosion, a series of soil and water conservation measures, including slope improvement and gully management, have been implemented in small watersheds [16]. The Zuli River Basin (ZRB) is a typical arid and semi-arid sub-basin of the Yellow River Basin in China. During the past century, severe soil erosion and complex changes in vegetation cover and hydrologic processes have been experienced due to climate change and complex man-made disturbances [17]. Therefore, there is a need to understand the patterns, main drivers, and impacts of vegetation cover in the ZRB. Therefore, the main contents of this study include: (1) assessing the spatial and temporal dynamics of vegetation cover from 1987 to 2020; (2) analyzing the relationship between NDVI and precipitation, temperature, and exploring the contribution rate of human activities and climate factors; and (3) studying the effects of vegetation cover change on runoff and sediment discharge.

## 2. Materials and Methods

### 2.1. Study Area Description

The Zuli River Basin (ZRB) is located in the northwestern part of China's Loess Plateau (Figure 1). The ZRB has a basin area of 10,647 km<sup>2</sup> and a river length of 220 km, and belongs to the Third and Fifth Sub-areas of the Loess hilly and gully region, which are warm in summer and cold and dry in winter. The annual soil erosion modulus is 4710 t/km<sup>2</sup>, and is mainly caused by the water erosion and gravity erosion, because the vegetation cover in the ZRB is low. A series of soil and water conservation measures, such as reservoirs and silt dams, have been built in the ZRB since the 1970s, and of engineering and vegetation measures has been used for gully slope management. In order to analyze the distribution of vegetation accurately, the whole watershed is divided into four parts: upstream Chankou, upstream Huining, middle stream, and downstream.

### 2.2. Data Sources

- (1) Satellite imagery: The datasets used in this study include Landsat 5 Surface Reflectance, Landsat 7 Surface Reflectance, Landsat 8 Surface Reflectance [18]. These data include properties such as cloud, shadow, water, and snow mask, and per-pixel saturation mask.
- (2) Climate data: TerraClimate combines WorldClim, CRU Ts4.0 and Japanese 55 year Reanalysis (JRA55) [19]. These datasets include precipitation, temperature, actual evapotranspiration, Palmer drought severity index, soil moisture, and so on.
- (3) Hydrological data: The runoff and sediment load data from 1987 to 2021 were provided by the Hydrology Department of Gansu Province.

### 2.3. Methods

#### 2.3.1. NDVI Calculation

The GEE provided the Landsat surface reflectance dataset, consisting of atmospherically corrected data from the Landsat 5 ETM, Landsat 7 ETM+ and Landsat 8 OLI/TIRS sensors. For this study, we analyzed 22,794 images. Firstly, the images were filtered ac-

ording to the pixel data quality of flag information. Then, the NDVI was calculated using Formula (1), and all of the images were combined and extracted.

$$\text{NDVI} = (\text{NIR} - \text{RED}) / (\text{NIR} + \text{RED}) \quad (1)$$

where NIR is surface reflectance in the near infrared band, and RED is the surface reflectance in the red band.

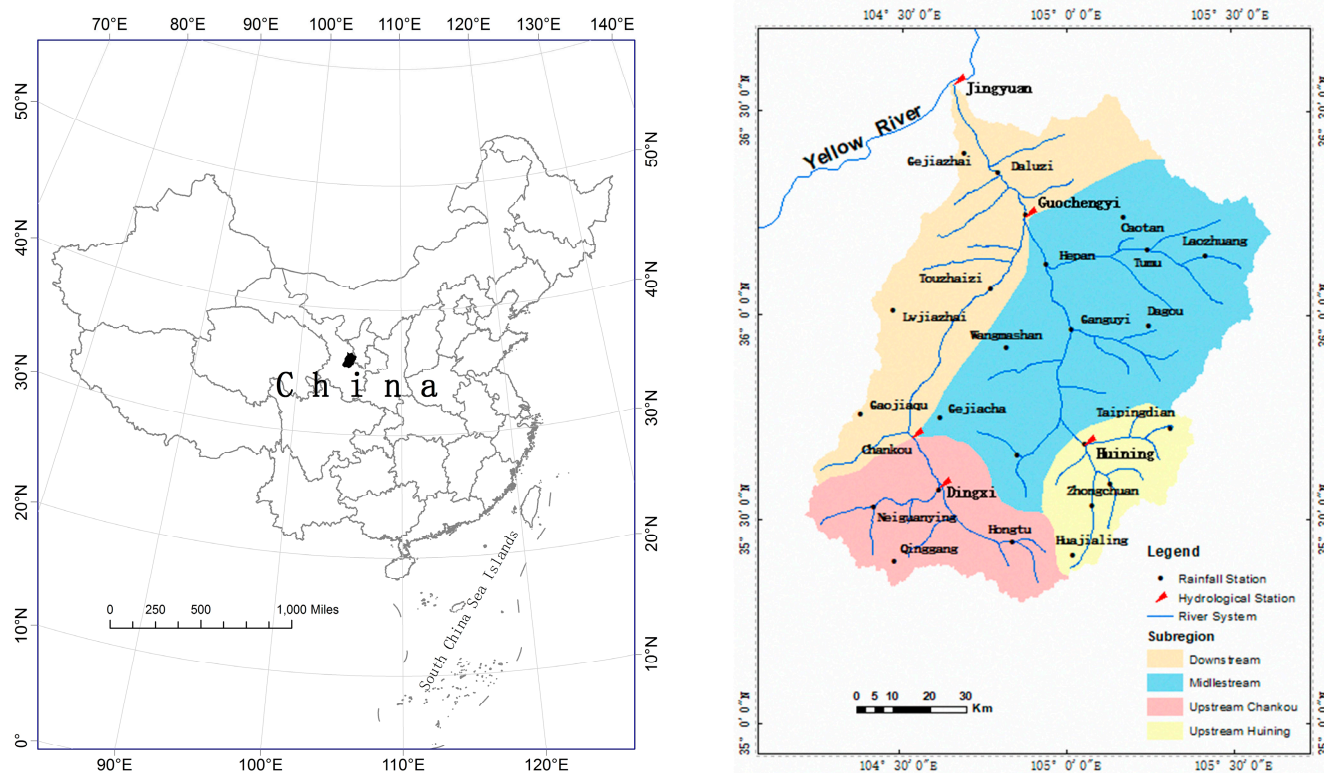


**Figure 1.** Location of the study area and stations in the Zuli River Basin.

### 2.3.2. Change Trend Detect

Mann–Kendall was used to identify the abrupt points [20]. The hyperbolic curve of the statistic  $U$  was obtained, and the intersection of the two curves denotes the mutation point. Sen's slope, which is widely used in hydro-meteorological time series analysis [21], was used to evaluate the trend of the sample data, and can be regarded as a proxy of land degradation/improvement [22]. Three categories of NDVI changes were defined, as follows: (i) significant increase (slope  $> 0$ ,  $p$ -value  $< 0.05$ ), no significant change (slope = 0,  $p$ -value  $> 0.05$ ) and significant decrease (slope  $< 0$ ,  $p$ -value  $< 0.05$ ). Additionally, we applied wavelet analysis using the F-test method to evaluate the relationship between vegetation cover, precipitation, runoff coefficient and sediment discharge.

### 2.3.3. Cumulative Slope Change Rate

The method for determining the cumulative slope change rate used in this study was to create a multiple linear regression equation between the NDVI and the climatic factors during the study period. This method was used to fit the NDVI throughout the whole study period, with the assumption that the NDVI sequence was only affected by climate change. The contribution rates of human activity and climate change to changes in NDVI were calculated using Formulas (3)–(6) [23].

$$R_1 = 100 \times (\text{slope}_b - \text{slope}_a) / \text{slope}_a \quad (2)$$

Among them,  $R_1$  is the slope change rate (%), and  $\text{slope}_a$  and  $\text{slope}_b$  are the values of NDVI before and after the mutation year.

$$R_2 = 100 \times (\text{slope}_{\text{fit-b}} - \text{slope}_{\text{fit-a}}) / \text{slope}_{\text{fit-a}} \quad (3)$$

$R_2$  is the slope change rate (%) of the cumulative fitting NDVI, and  $\text{slope}_{\text{fit-a}}$  and  $\text{slope}_{\text{fit-b}}$  are the values of NDVI fitted using the multivariate linear model before and after the mutation year.

$$C_C = 100 \times R_1 / R_2 \quad (4)$$

In Formula (4),  $C_C$  is the contribution rate of climate change to NDVI change.

$$C_H = 100 - C_C \quad (5)$$

In Formula (5),  $C_H$  is the contribution rate of human activity to NDVI change.

#### 2.3.4. Wavelet Analysis

Wavelet analysis was used to measure the local correlation of two time series in time–frequency space [24], highlighting the relationship between the NDVI index and hydrological elements in the high-energy region in the time–frequency domain. To date, these kinds of methods have been widely used in the field of geophysics and hydrology. The cross wavelet transform can detect the time-domain and frequency-domain variations and coupling oscillations of two given time series. The coherent wavelet transform focuses on the correlation of low-energy regions, which is used to measure the local correlation of two time series in time–frequency space [25]. A wavelet packet is provided in MATLAB.

### 3. Results

#### 3.1. Temporal Change in NDVI

The maximum yearly NDVI in the ZRB was extracted from 30 m satellite images based on GEE during the period between 1987 and 2021 (Figure 2). The results showed that the multi-year average NDVI for the ZRB was 0.2051 between 1987 and 2021, with the NDVI in the upper reaches of the ZRB being the greatest, while the multi-year average NDVI in the reaches above Chankou and above Huining were 0.2504 and 0.2344, respectively, and the NDVI in the middle and lower reaches of the basin was lower, at 0.1950 and 0.1811, respectively.

With respect to the change trend, the annual maximum NDVI in the study area increased from 1987 to 2021, and the rate of increase of NDVI in the upstream reaches of the ZRB was evidently higher than that in other parts of the catchment. Specifically, from 1987 to 2021, the change slopes of NDVI at Upstream\_Chankou and Upstream\_Huining were 0.0044/a and 0.0048/a, respectively, values which are slightly higher than the NDVI change slope for the whole catchment (0.004/a), and the midstream and downstream NDVI change slopes (0.0039/a and 0.0038/a, respectively). Since the afforestation commenced in 1999, the variation trend of NDVI in the ZRB has increased, especially in the middle reaches of the Zuli River. This is associated with the implementation of soil and water conservation measures in the midstream areas. Meanwhile, the change gradient of NDVI in the upstream Chankou and upstream Huining areas is still the largest, both with a value of 0.0079/a.

#### 3.2. Spatial Pattern of NDVI Dynamics

In terms of the spatial distribution of NDVI, there is a strong spatial heterogeneity with respect to vegetation cover; NDVI increased from north to the south, changing from 0.15 in the lower reaches to 0.54 in the upper reaches. High values occur in the upstream reaches, as well as in the middle and lower reaches of the southeastern edge of the region. In contrast, lower NDVI values were found in the middle and other downstream parts of the ZRB (Figure 3a).

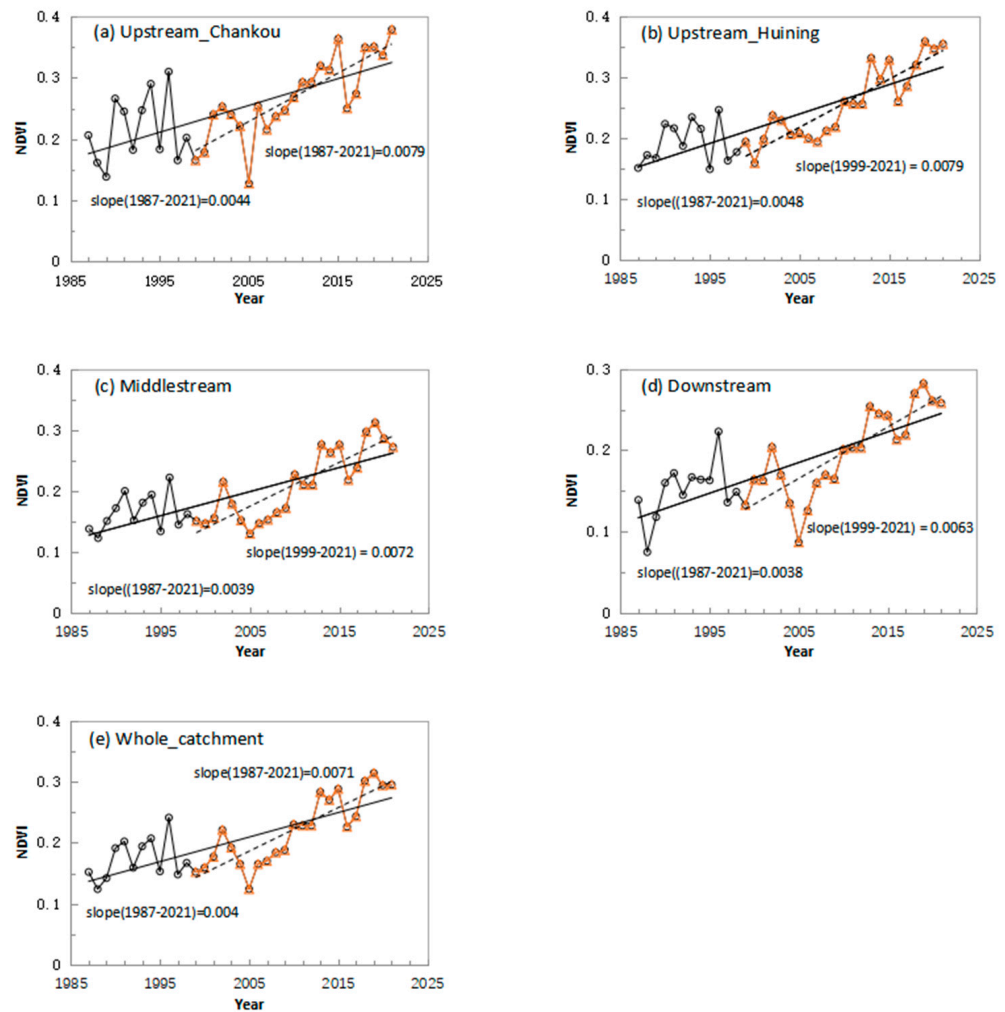


**Figure 2.** Interannual change in the annual maximum NDVI in different parts of the ZRB from 1987 to 2021.

From Figure 3b, it can be seen that the NDVI values corresponding to most areas of the ZRB show an increasing trend, with a change slope between 0 and 0.022/a. The areas with a decreasing trend of NDVI are distributed in the river channel of the basin, with a corresponding relative change rate below 0%, and reaching a value as high as nearly 30% in the upstream channel region (Figure 3c).

Further statistical analysis showed that most areas (95% of whole area) were characterized by significantly increased NDVI during the period 1987–2021 (Figure 3d). The significantly reduced area only accounted for 0.07% of the study area, distributed in the upstream river channel, while there was no significant change in the rest of the areas.

### 3.3. Relationship between NDVI and Climate Factors

The hydrometeorological conditions in different parts of the ZRB changed dramatically between 1956 and 2021, especially in cases where there was a significant decrease in annual precipitation. In order to evaluate the hydrometeorological conditions and human activities occurring in recent years, wavelet analysis was used in this study.

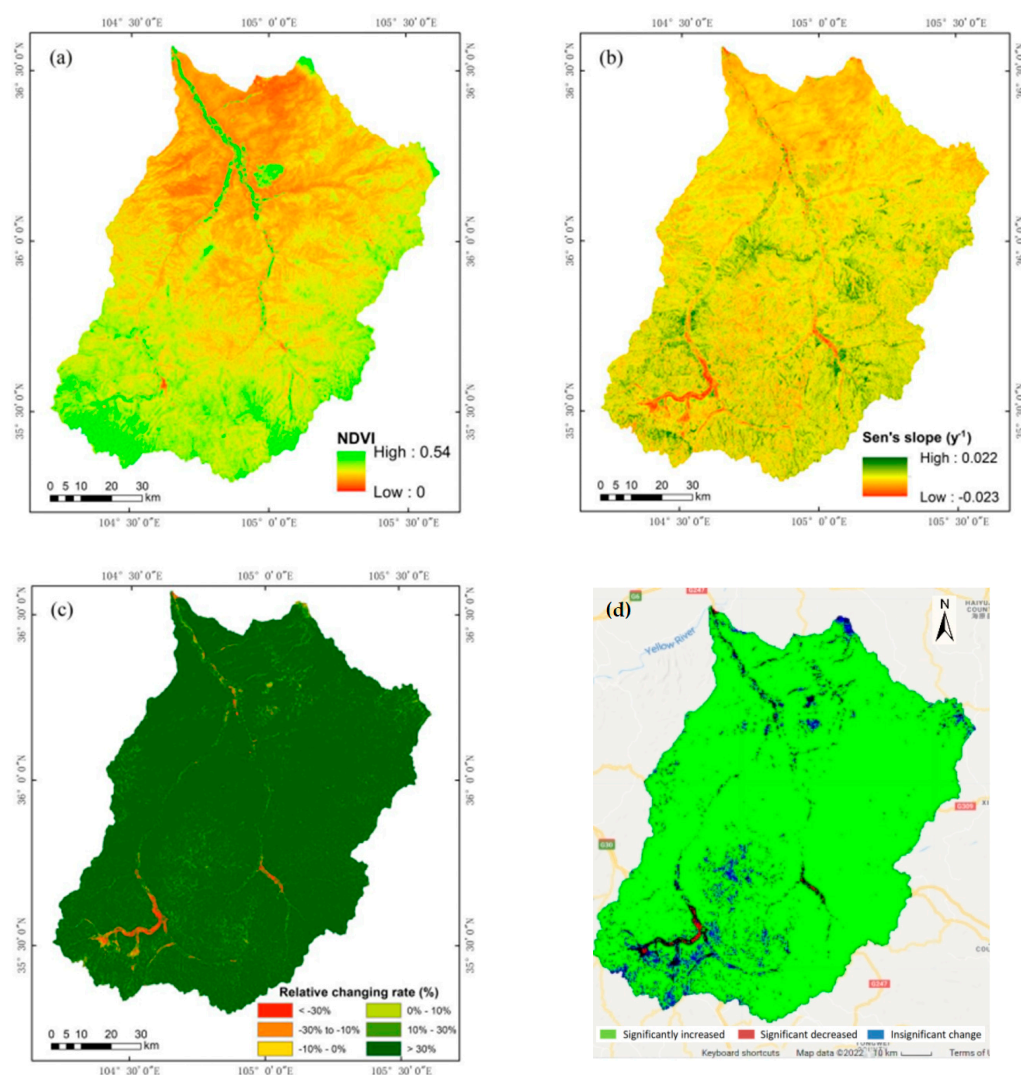


**Figure 3.** Spatial pattern of the mean annual NDVI (a), Sen's slope of mean annual NDVI (b) and Relative changing rate of mean annual NDVI (c) in different parts of the ZRB from 1987 to 2021. Figure (d) refer to the significant change of mean annual NDVI of the ZRB during 1987–2021, in figure (d), the blue represents no significant change, green represents a significant increase, and red represents a significant decrease.

### 3.3.1. Climate Change Trend

For the period from 1987 to 2021, the average precipitation, temperature, actual evapotranspiration, and soil moisture in the ZRB were 372.1 mm, 11.17 °C, 40.16 mm, and 10.08 mm, respectively. From 1987 to 2021, the climate factors in the ZRB showed an increasing trend. The precipitation, temperature, actual evapotranspiration, and soil moisture increased by 0.7918/a, 0.0249/a, 0.0626/a, and 0.1487/a, respectively (Figure 4).

### 3.3.2. Contribution Rate of Climate Factors and Human Activities to NDVI

We evaluated the contribution rates of climate factors and human activities to NDVI during the period between 1987 and 2021 using the cumulative slope change rate method. The results showed that the contribution rates of climatic factors and human activities to the dynamic changes in NDVI in the ZRB from 1987 to 2021 were 38.32% and 61.68%, respectively, with human activities being the main factors causing changes in NDVI (Figure 5).

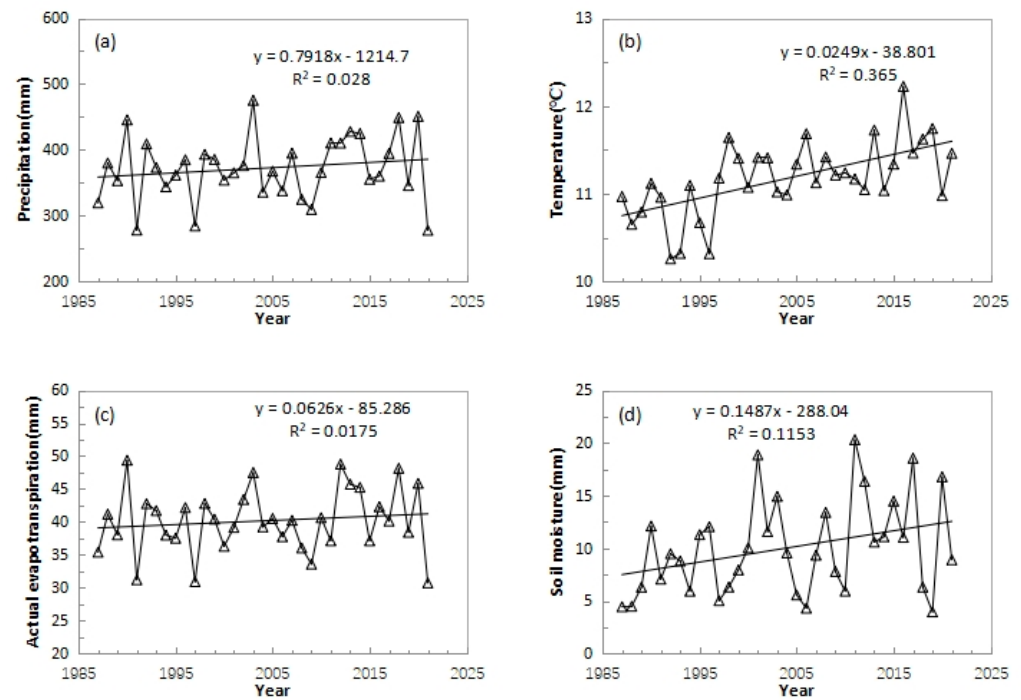


**Figure 4.** Interannual variations of climate factors in the ZRB from 1987 to 2021. (a) is the sum precipitation change in the ZRB during 1987–2021; (b) is the average temperature change in the ZRB during 1987–2021; (c) is the average actual evapotranspiration change in the ZRB during 1987–2021; (d) is the average soil moisture change in the ZRB during 1987–2021.

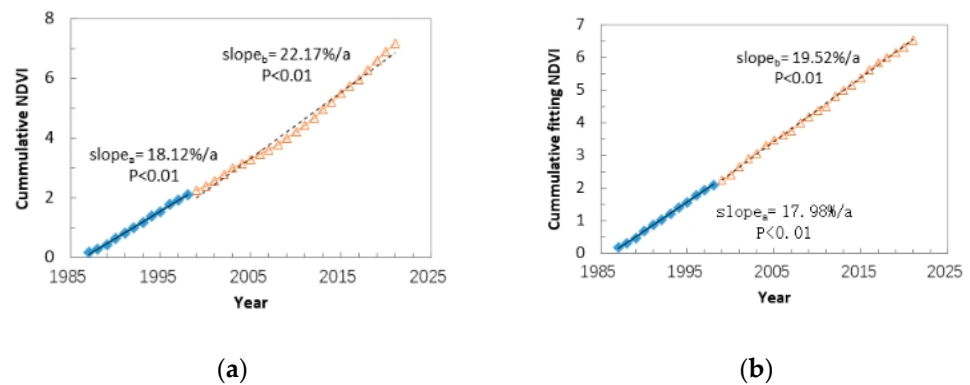


**Figure 5.** Linear relationship between year and cumulative NDVI and cumulative fitting NDVI. (a) refer to the cumulative NDVI change situation before and after 1999 in the ZRB from 1987–2021. (b) show the values of NDVI fitted using the multivariate linear model before and after the mutation year.

### 3.4. Relationship between NDVI and Runoff and Sediment

#### 3.4.1. Runoff and Sediment Concentration

The average annual runoff of the ZRB from 1987 to 2021 was  $0.34 \times 10^8 \text{ m}^3$ , showing a significant decreasing trend. Among the different areas, the annual average runoff in the downstream reaches was the highest, at  $0.82 \times 10^8 \text{ m}^3$ , and the decrease was the greater, with a gradient of runoff change of  $-0.015/\text{a}$ . The runoff above Huining was the smallest, with values between 0 and  $0.2 \times 10^8 \text{ m}^3$ , with an average value of  $0.08 \times 10^8 \text{ m}^3$ . The annual average runoff values in the areas above the mouth and in the middle reaches were  $0.26 \times 10^8 \text{ m}^3$  and  $0.20 \times 10^8 \text{ m}^3$ , respectively, with change slopes of  $-0.0038/\text{a}$  and  $-0.0016/\text{a}$ , respectively (Figure 6).

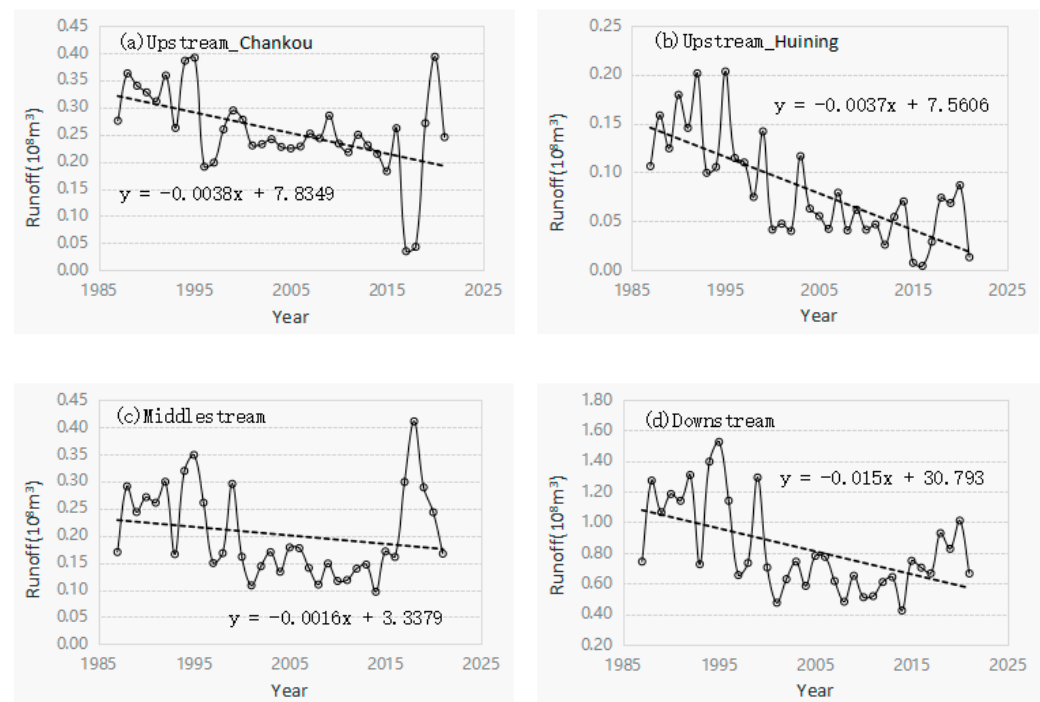


**Figure 6.** The interannual variation of annual runoff in Upstream\_Chankou (a), Upstream\_Huining (b), Middlestream (c) and Downstream (d) of the ZRB from 1987 to 2021.

The average annual sediment of the ZRB from 1987 to 2021 was  $846.35 \times 10^4$  t, showing a significant decreasing trend. Among the different areas, the runoff in the downstream reaches was the highest, at  $2299.14 \times 10^4$  t, and the decrease was the greatest, with a gradient of runoff change of  $-126.71/a$ . The sediment load above Huining was the lowest, with values between  $0.32$  and  $676 \times 10^4$  t, with an average value of  $176.43 \times 10^4$  t. The sediment load above Chankou was similar to that of Huining, with a multi-year average of  $196.09 \times 10^4$  t. The change slopes of the two upstream areas were similar, and the values above Chankou and Huining were  $-10.813/a$  and  $-17.888/a$ , respectively. The amount of sediment in the midstream area was much smaller than that in the downstream reaches, but larger than that in the upstream area, with an average value of  $713.76 \times 10^4$  t and a change slope of  $-29.484/a$  (Figure 7).

### 3.4.2. Runoff Coefficient and Sediment Concentration Change with NDVI

The value of NDVI is related to the runoff coefficient and sediment concentration. The NDVI in 1988–1993 and 1994–1999 showed a significant negative change, with a signal of 2–4 years and 1–2 years, respectively, in the upstream Chankou area (Figure 8A,B), but there was no significant change in NDVI, because runoff coefficient was also influenced by climate factors. There was also a significant negative correlation ( $p < 0.05$ ) between the signals from 1991 to 1997 in the upstream Huining area (Figure 8C,D). Similarly, the results show that in the downstream reaches of the ZRB, the signal for NDVI and runoff coefficient was 4–6 years in 1998–2002 (Figure 8G,H). However, the NDVI and runoff coefficient show a positive correlation with 2–3.5 years in the 1998–2002 in the middlestream area of the ZRB (Figure 8E,F).

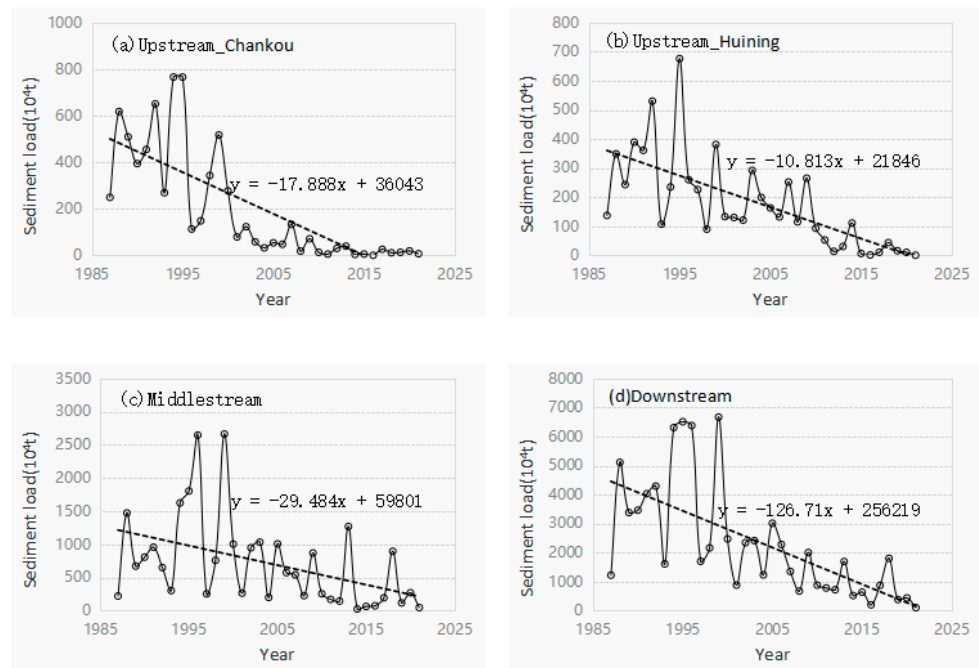


Figure 7. The interannual changes in annual sediment load in Upstream\_Chankou (a), Upstream\_Huining (b), Middlestream (c) and Downstream (d) of the ZRB from 1987 to 2021.

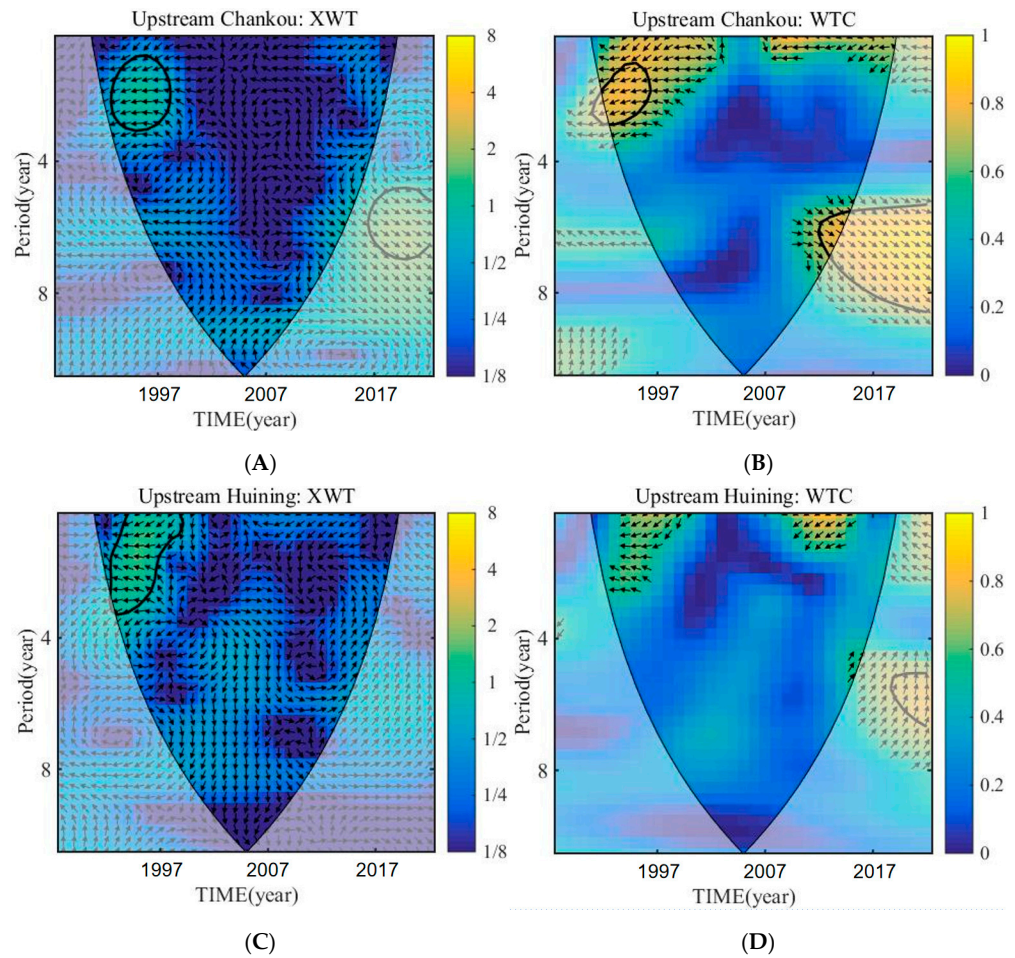
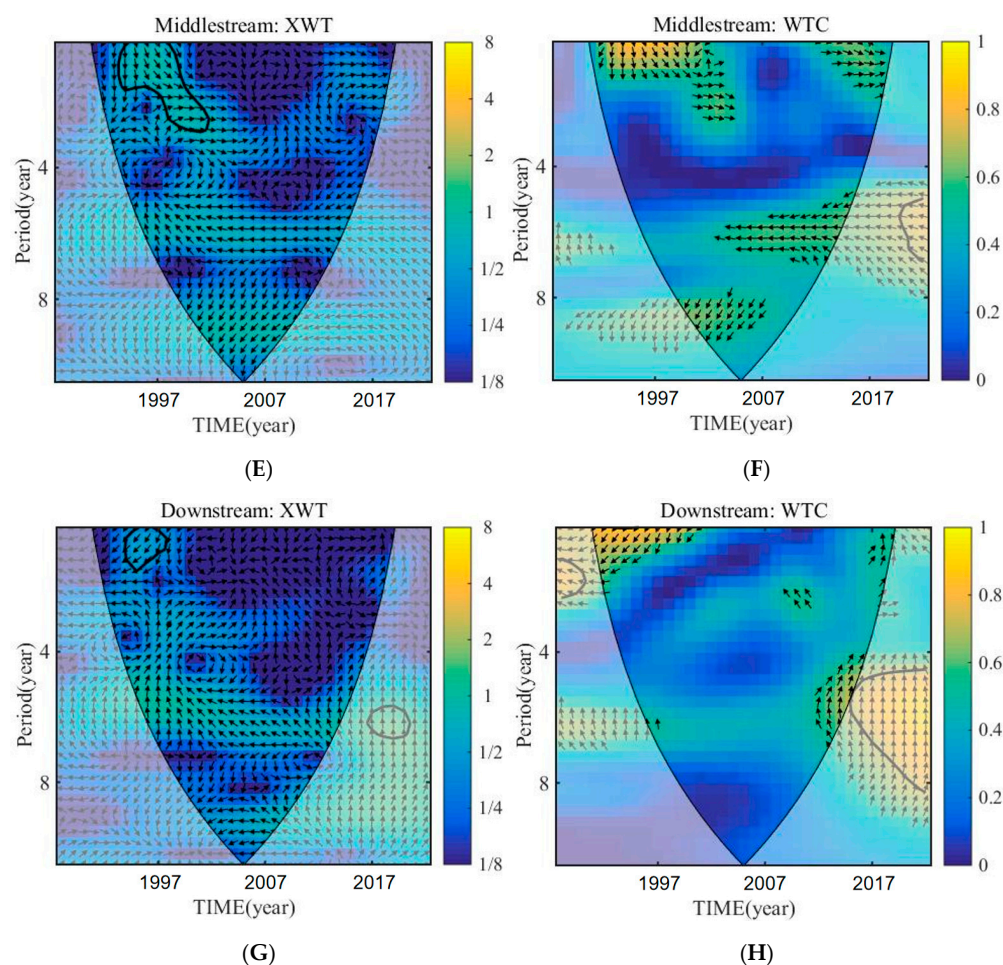
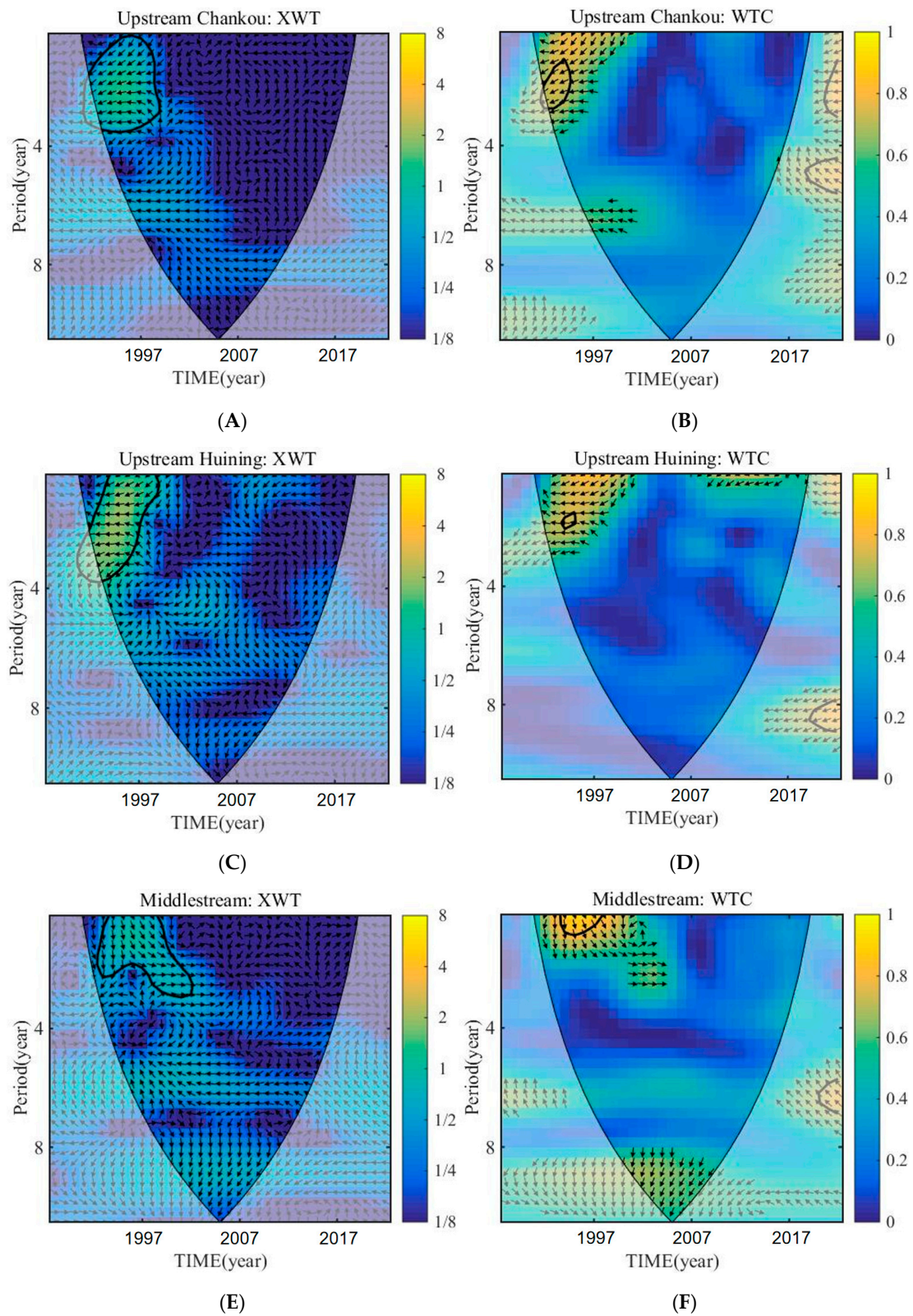


Figure 8. Cont.



**Figure 8.** The relationship between annual maximum NDVI and runoff coefficient in the upstream Chankou (A,B), upstream Huining (C,D), middlestream (E,F) and Downstream (G,H) of the ZRB.

The correlation between NDVI and sediment was negative, ranging from 2 to 3.5 years in 1988–1993 and 0.5 to 3.5 years in 1994–1997 (Figure 9A,B) in the area upstream of Chankou, a signal of 1–2 years in 1994–1996. For the upstream Huining, there is also significant negative correlation ( $p < 0.05$ ) with 1–3 years of signal from 1991–1997 (Figure 8C,D), and a signal of 0.5–3 years for NDVI and sediment concentration from 2012 to 2021 in the middlestream area of the ZRB (Figure 8E,F), respectively. For the downstream area of the ZRB, NDVI was significantly positively correlated with sediment concentration ( $p < 0.05$ ), with a signal of 1–4 years from 1996 to 2001 (Figure 8G,H).

**Figure 9.** *Cont.*

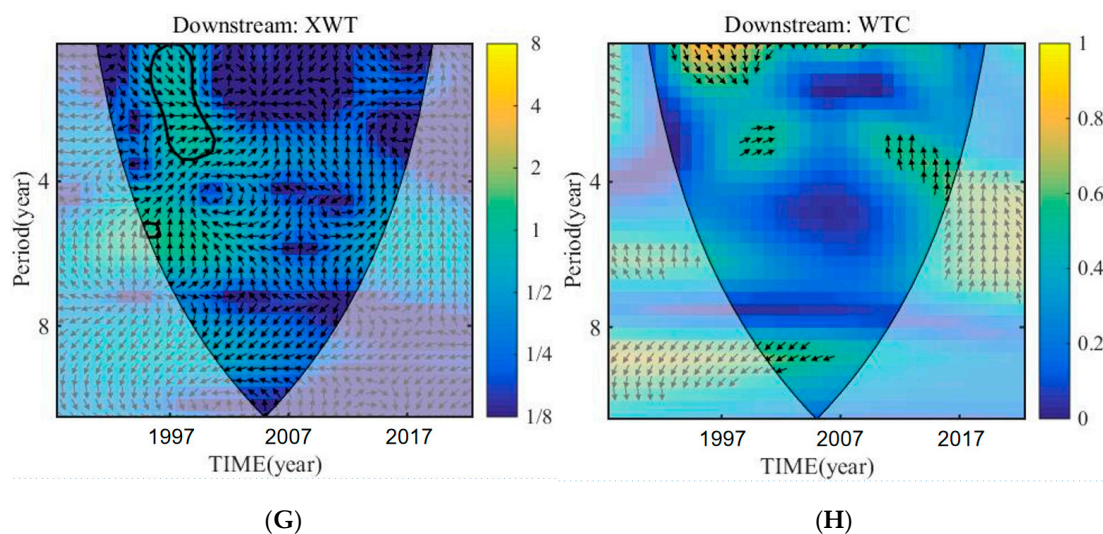


**Figure 9.** The relationship between annual maximum NDVI and sediment load in the upstream Chankou (A,B), upstream Huining (C,D), middlestream (E,F) and Downstream (G,H) of the ZRB.

#### 4. Discussion

Dynamic monitoring of vegetation cover is an important link in the process of adjusting the balance of terrestrial ecosystems and climate systems. This study used the GEE to extract annual maximum NDVI at 30 m for the growing season; the relationship between NDVI and precipitation, runoff coefficient, and sediment concentration across the ZRB during the period 1987–2021 were also discussed.

##### 4.1. NDVI Variation

NDVI showed an upward trend from 1987 to 2021, and there were significant differences in the annual average NDVI values in different parts of the catchment. Although NDVI in the upstream Chankou and upstream Huining reaches was higher than that in the middle and lower reaches, the growth rate of the NDVI in the upstream reaches was lower than that in other parts of the ZRB. Before the implementation of GPP, the NDVI only exhibited small changes (i.e., no significant change), while after the implementation of GPP, vegetation cover generally increased. There was a significant correlation ( $p < 0.05$ ) between precipitation and NDVI in the upstream Huining and middle stream before 2002. However, due to the influence of human activities, this effect has gradually weakened since 2002. The areas upstream of Chankou were hardly affected by any significant precipitation. However, for downstream areas, the impact of precipitation on NDVI continued until 2012, as the soil and water conservation measures were implemented later, while soil and water conservation measures in downstream areas were less significant. At the same time, human activity is also considered to be an important factor in helping to reduce runoff and sediment.

In some areas of the lower reaches of the ZRB, as well as in the river valley, especially in the urban area of Dingxi and in Huining county, the slope of NDVI is negative, indicating that urban expansion has a negative impact on NDVI, but the urban area accounts for only a small proportion of the watershed area, and therefore the impact on the overall NDVI variation in the basin is limited. Therefore, it is important to study the causes and effects of NDVI change under global environmental changes and man-made disturbances in order to better formulate soil and water conservation measures.

##### 4.2. The Causes and Consequences of Changes in Vegetation Coverage

The vegetation cover has been affected by both climate change and human activities. The contribution rates of climatic factors and human activities to the dynamic changes in vegetation index were 38.32% and 61.68%, respectively, in the ZRB from 1987 to 2021. This

is consistent with most studies. For example, Gbenga et al. [26] found a relatively minor ( $R < 0.5$ ) relationship between NDVI3g and climatic variables, with seasonal fluctuations in different vegetation types. Darius et al. [27] found that land cover change in Zambia was influenced by factors such as forest losses, conservation status (national forests), population density, and physical proximity to facilities between 1972 and 2016. Mingguo Ma et al. [28] showed that the effect of precipitation on vegetation cover in mountain areas is greater than that in oasis areas. Precipitation also exerts a lagged effect on MNDVI, especially in the mountainous areas of the Heihe River Basin, with an annual recurrence.

Affected by natural factors and human activities, the underlying surface of the basin has changed. Changes in vegetation cover not only reflect the trend of ecological environmental change in the river basin, they also imply a certain response to the runoff and sediment in the river basin. Vegetation cover changes are coupled with a variety of factors that exhibit spatial differences, and the hydrological effects caused by them are more complex [29]. Studies have shown that NDVI and flood peak discharge are mostly negatively correlated. In areas with higher vegetation coverage, the effect on flood peaks is reduced to a certain extent. This is basically consistent with the results obtained in this paper. In 1988–1993 and 1994–1999, the upper reaches of Gukou had a significant negative correlation of 2–4 years and 1–2 years, respectively, the upper reaches of Huining had a significant negative correlation with NDVI in 1991–1997, and the downstream area had a significant negative correlation between 1998 and 2002. There was a significant negative correlation between 4 and 6 years, and the runoff flow in the corresponding time period in these regions was higher than the average level, with increasing vegetation leading to an increase in the interception of runoff.

From 1998 to 2002, NDVI and runoff in the midstream showed a positive correlation. Analysis showed that afforestation activities in 1999 caused a significant increase in NDVI. The increase in NDVI increases the amount of water vapor evaporated into the air, and the precipitation falls to the ground with the movement of the atmosphere, leading to an increase in runoff, which is evaporated into the air. Thus, the amount of water vapor increases, and as the atmosphere moves, precipitation falls to the ground, allowing vegetation to grow vigorously. Another explanation is that NDVI has a positive correlation with dry runoff, and the increase in vegetation coverage significantly increases runoff during the dry season.

## 5. Conclusions

Based on GEE, this study analyzed the spatiotemporal changes, driving factors and influences of the NDVI in the ZRB. The conclusions are as follows:

The multi-year average NDVI of the ZRB was 0.2051 from 1987 to 2021. In addition, the NDVI in the upstream of the ZRB was the highest, with the multi-year average NDVI above Chankou and above Huining being 0.2504 and 0.2344, respectively, and the NDVI in the middle and lower reaches of the basin was lower, at 0.1950 and 0.1811, respectively.

NDVI in the ZRB showed a significant increasing trend (0.004/a). The growth rates of NDVI in the Upsteam\_Chankou and Upstream\_Huining were 0.0044/a and 0.0048/a, respectively. The midstream and downstream NDVI change slopes were 0.0039/a and 0.0038/a, respectively. With respect to spatial distribution, the NDVI in the study area has obvious spatial heterogeneity. The high values are distributed in the upstream ZRB, low NDVI values in other parts of the middle and downstream areas of the ZRB.

The precipitation, temperature, actual evapotranspiration, and soil moisture are the three main driving climate factors that affect NDVI. After 1999, due to the measures implemented to return farmland to forests and grassland, the impact of human activities on vegetation has gradually become a positive one. Of the ZRB, 38.32% and 61.68% have been positively affected by climate factors and human activities, respectively.

The average annual runoff and sediment load of the ZRB from 1987 to 2021 both showed a significant decreasing trend. The upstream and downstream NDVI and runoff showed a significant negative correlation in a certain period of time, and the midstream

showed a significant positive correlation. Upstream and midstream NDVI was significantly negatively correlated with sediment volume, and downstream NDVI was significantly positively correlated.

**Author Contributions:** Conceptualization, C.H. and J.X.; methodology, C.H. and L.S.; software, C.H.; validation, C.H., J.X. and L.S.; formal analysis, C.H.; data curation, C.H. and L.S.; writing—original draft preparation, C.H.; writing—review and editing, C.H. and J.X.; visualization, C.H. and L.S.; supervision, J.X. All authors have read and agreed to the published version of the manuscript.

**Funding:** This research was funded by Gansu Province Water Conservancy Science Experiment Research and Technology Promotion Project, grant number Ganshui Jianguanfa [2021] No. 71.

**Institutional Review Board Statement:** Not applicable.

**Informed Consent Statement:** Not applicable.

**Data Availability Statement:** Not applicable.

**Acknowledgments:** The author is grateful to the editor and anonymous reviewers for spending their valuable time on constructive comments and suggestions that improved the quality of the manuscript considerably.

**Conflicts of Interest:** The authors declare no conflict of interest.

## References

- Li, A.; Wu, J.; Huang, J. Distinguishing between human-induced and climate-driven vegetation changes: A critical application of RESTREND in inner Mongolia. *Landsc. Ecol.* **2012**, *27*, 969–982. [[CrossRef](#)]
- Xin, Z.B.; Xu, J.X.; Zheng, W. Spatiotemporal variations of vegetation cover on the Chinese Loess Plateau (1981–2006): Impacts of climate changes and human activities. *Sci. China Ser. D Earth Sci.* **2008**, *51*, 67–78. [[CrossRef](#)]
- Du, J.Q.; Shu, J.M.; Yin, J.Q.; Yuan, X.J.; Jiaerheng, A.; Xiong, S.S.; He, P.; Liu, W.L. Analysis on spatio-temporal trends and drivers in vegetation growth during recent decades in Xinjiang, China. *Int. J. Appl. Earth Obs. Geoinf.* **2015**, *38*, 216–228. [[CrossRef](#)]
- Pang, G.; Wang, X.; Yang, M. Using the NDVI to identify variations in, and responses of, vegetation to climate change on the Tibetan Plateau from 1982 to 2012. *Quat. Int.* **2017**, *444*, 87–96. [[CrossRef](#)]
- Fang, W.; Huang, S.; Huang, Q.; Huang, G.; Meng, E.; Luan, J. Reference evapotranspiration forecasting based on local meteorological and global climate information screened by partial mutual information. *J. Hydrol.* **2018**, *561*, 764–779. [[CrossRef](#)]
- Wen, X.; Wang, Q.; Zhang, G.; Bai, J.; Wang, W.; Zhang, S. Assessment of heavy metals contamination in soil profiles of roadside Suaeda salsa wetlands in a Chinese delta. *Phys. Chem. Earth* **2017**, *97*, 71–76. [[CrossRef](#)]
- Chu, H.; Venevsky, S.; Wu, C.; Wang, M. NDVI-based vegetation dynamics and its response to climate changes at Amur-Heilongjiang River Basin from 1982 to 2015. *Sci. Total Environ.* **2019**, *650*, 2051–2062. [[CrossRef](#)]
- Robinson, N.P.; Allred, B.W.; Jones, M.O.; Moreno, A.; Kimball, J.S.; Naugle, D.E.; Erickson, T.A.; Richardson, A.D. A dynamic landsat derived normalized difference vegetation index (NDVI) product for the conterminous United States. *Remote Sens.* **2017**, *9*, 863. [[CrossRef](#)]
- Zhao, A.; Zhang, A.; Liu, J.; Feng, L.; Zhao, Y. Assessing the effects of drought and “Grain for Green” Program on vegetation dynamics in China’s Loess Plateau from 2000 to 2014. *Catena* **2019**, *175*, 446–455. [[CrossRef](#)]
- Bao, G.; Qin, Z.; Bao, Y.; Zhou, Y.; Li, W.; Sanjiv, A. NDVI-based long-term vegetation dynamics and its response to climatic change in the Mongolian plateau. *Remote Sens.* **2014**, *6*, 8337–8358. [[CrossRef](#)]
- Huang, C.; Yang, Q.; Huang, W.; Zhang, J.; Li, Y.; Yang, Y. Hydrological response to precipitation and human activities—A case study in the Zuli River basin, China. *Int. J. Environ. Res. Public Health* **2018**, *15*, 2780. [[CrossRef](#)] [[PubMed](#)]
- Zhang, L.; Wang, J.; Bai, Z.; Lv, C. Effects of vegetation on runoff and soil erosion on reclaimed land in an opencast coal-mine dump in a loess area. *Catena* **2015**, *128*, 44–53. [[CrossRef](#)]
- Duan, L.; Huang, M.; Zhang, L. Differences in hydrological responses for different vegetation types on a steep slope on the Loess Plateau, China. *J. Hydrol.* **2016**, *537*, 356–366. [[CrossRef](#)]
- McVicar, T.R.; Li, L.T.; Van Niel, T.G.; Zhang, L.; Li, R.; Yang, Q.K.; Zhang, X.P.; Mu, X.M.; Wen, Z.M.; Liu, W.Z.; et al. Developing a decision support tool for China’s re-vegetation program: Simulating regional impacts of afforestation on average annual streamflow in the Loess Plateau. *For. Ecol. Manag.* **2007**, *251*, 65–81. [[CrossRef](#)]
- Liu, Y.; Lei, H. Responses of natural vegetation dynamics to climate drivers in China from 1982 to 2011. *Remote Sens.* **2015**, *7*, 10243–10268. [[CrossRef](#)]
- Cao, Z.; Li, Y.R.; Liu, Y.S.; Chen, Y.F.; Wang, Y.S. When and where did the Loess Plateau turn “green”? Analysis of the tendency and breakpoints of the normalized difference vegetation index. *Land Degrad. Dev.* **2018**, *29*, 162–175. [[CrossRef](#)]
- Yao, B.; Liu, Q. Characteristics and influencing factors of sediment deposition-scour in the Sanhuhekou-Toudaoguai Reach of the upper Yellow River, China. *Int. J. Sediment Res.* **2018**, *33*, 303–312. [[CrossRef](#)]

18. USGS. *Landsat Surface Reflectance Data*; USGS EROS: Sioux Falls, SD, USA, 2015.
19. Abatzoglou, J.T.; Dobrowski, S.Z.; Parks, S.A.; Hegewisch, K.C. TerraClimate, a high-resolution global dataset of monthly climate and climatic water balance from 1958–2015. *Sci. Data* **2018**, *5*, 170–191. [[CrossRef](#)]
20. Sneyers, R. *On the Statistical Analysis of Series of Observations*; World Meteorological Organization: Geneva, Switzerland, 1990; p. 415.
21. Tabari, H.; Somee, B.S.; Zadeh, M.R. Testing for long-term trends in climatic variables in Ira. *Atmos* **2011**, *100*, 1–132.
22. Sen, P.K. Estimates of the Regression Coefficient Based on Kendall’s Tau. *J. Am. Stat. Assoc.* **1968**, *63*, 1379–1389. [[CrossRef](#)]
23. Peng, Y.; Li, F.; Xu, N.; Kulmatov, R.; Gao, K.; Wang, G.; Zhang, Y.; Qiao, Y.; Li, Y.; Yang, H.; et al. Spatial-temporal variations in drought conditions and their climatic oscillations in Central Asia from 1990 to 2019. *Chin. J. Eco-Agric.* **2021**, *29*, 312–324.
24. Wang, Y.; Song, G.; Li, W. The interaction relationship between land use patterns and socioeconomic factors based on wavelet analysis: A case study of the black soil region of Northeast China. *Land* **2021**, *10*, 1237. [[CrossRef](#)]
25. Torrence, C.; Compo, G.P. A Practical Guide to Wavelet Analysis. *Bull. Am. Meteorol. Soc.* **1998**, *79*, 61–78. [[CrossRef](#)]
26. Gobena, A.K.; Gan, T.Y. The role of pacific climate on low-frequency hydroclimatic variability and predictability in Southern Alberta, Canada. *J. Hydrometeorol.* **2009**, *10*, 1465–1478. [[CrossRef](#)]
27. Phiri, D.; Morgenroth, J.; Xu, C. Long-term land cover change in Zambia: An assessment of driving factors. *Sci. Total Environ.* **2019**, *697*, 134206. [[CrossRef](#)] [[PubMed](#)]
28. Ma, M.; Frank, V. Interannual variability of vegetation cover in the Chinese Heihe River Basin and its relation to meteorological parameters. *Int. J. Remote Sens.* **2006**, *27*, 3473–3486. [[CrossRef](#)]
29. Appels, W.M.; Bogaart, P.W.; van der Zee, S.E.A.T.M. Influence of spatial variations of microtopography and infiltration on surface runoff and field scale hydrological connectivity. *Adv. Water. Resour.* **2011**, *34*, 303–313. [[CrossRef](#)]

**Disclaimer/Publisher’s Note:** The statements, opinions and data contained in all publications are solely those of the individual author(s) and contributor(s) and not of MDPI and/or the editor(s). MDPI and/or the editor(s) disclaim responsibility for any injury to people or property resulting from any ideas, methods, instructions or products referred to in the content.